Journal of Physics: Conference Series **2893** (2024) 012033
doi:10.1088/1742-6596/2893/1/012033

CFD simulation of the increased electric boost effects on the glass melting process in a real glass furnace to support decarbonisation of glass industry

Carlo Cravero[1], Davide Marsano[1*] and Gabriele Milanese[1]

[1] Dipartimento di Ingegneria Meccanica, Energetica, Gestionale e dei Trasporti (DIME), Università degli Studi di Genova, Via Montallegro 1, 16145 Genoa, Italy

[*]E-mail: davide.marsano@unige.it

Abstract. The glass industry plays a pivotal role in modern manufacturing, providing essential materials for a multitude of applications ranging from construction to consumer goods. However, the substantial energy demands, primarily driven by the intense heat required to melt raw materials within furnaces, pose significant challenges. Traditionally, thermal energy is sourced from combustion processes in dedicated chambers. Yet, in the pursuit of efficiency and environmental sustainability, there is a growing preference for integrated systems. Notably, the utilization of electrode installations within glass baths emerges as a promising choice for direct melting augmentation through electricity in a more efficient way. This study introduces a sophisticated computational fluid dynamics (CFD) model, developed by the authors, tailored to simulate the real operation of a glass furnace. The model fully couples the reactive flow in the combustion space (the furnace) with convective motions within the glass tank including the effect of the electrodes. By changing the thermal energy from combustion with varying levels of electrode operation (keeping the same overall heat flux to the glass), the furnace behaviour is investigated. The research specifically examines the effects of electrode operation on crucial furnace parameters, including flame heat release and convective motions inside the glass bath, across different scenarios. Insights are gained into the complex interplay between electrode operation, thermal dynamics, and glass quality within the furnace environment. The findings of this study not only deepen the understanding of fundamental processes within glass manufacturing but also offer actionable insights for industry stakeholders. By elucidating the intricate relationship between electrode operation and glass melting process, this research provides practical guidance for optimizing furnace design and operation, enhancing efficiency and CO2 reduction, with the same product quality, in the glass industry.

1. Introduction

The glass industry is a significant contributor to industrial carbon emissions, primarily due reliance on fossil fuels for the high-temperature processes required in glass melting. Notably, the energy demand of a glass furnace requires over 1500 [K] for the raw material melting process. Recent estimations within the European Union indicate that the glass industry consumes an average of 7.8 [GJ] annually, with a corresponding emission of 0.57 tons of CO_2 per ton of saleable product [1]. In the current global landscape, marked by increasingly stringent regulations on energy consumption and greenhouse gas emissions, the optimization of glass production systems becomes strategically imperative. A typical glass furnace comprises a combustion space and a glass tank, where fuel and combustion air interact to generate significant thermal energy through radiation and convection. Simultaneously, raw materials enter the glass tank, undergoing chemical reactions, fusion, and homogenization over several hours before exiting the furnace.

The urgent need to reduce carbon footprints has driven extensive research into alternative methods that can decarbonize glass production while maintaining efficiency and product quality. Various strategies have been implemented to mitigate the environmental impact of glass manufacturing. These include the adoption of regenerative or recuperative chambers [2], systems for preheating raw materials [3], exhaust gas recirculation systems [4], and air staging approaches to minimize specific emissions like NOx [5,6]. One promising approach is the utilization of electric boosting in glass furnaces [7], which involves the use of electrical energy through electrodes as a cleaner alternative to traditional fossil fuels. Electric boosting is an established technology that introduces electric currents directly into the glass melt, increasing the temperature, improving the melting efficiency and enhancing the convective recirculation of melted glass. This technique has been progressively optimized to reduce energy consumption and carbon emissions.

Recent studies have demonstrated the effectiveness of electric boosting in enhancing the melting rate and reducing the overall energy demand. For instance, Verheijen et al. [8] showed that electric boosting could significantly decrease CO_2 emissions by substituting a portion of the fossil fuel energy input with electric energy. Moreover, advancements in electrode materials and design have led to improved efficiency and longevity of electric boosting systems, as highlighted by Abenojar et al. [9]. CFD simulations have become an invaluable tool in analysing the complex thermal and fluid dynamics within glass furnaces. They offer detailed insights into temperature distribution, flow patterns, and heat transfer mechanisms, enabling the optimization of furnace design and operation. Notable work by Müller et al. [10] utilized CFD to model the impact of various boosting configurations on glass melt homogeneity and energy efficiency. Their findings underscored the potential of CFD in predicting the outcomes of process modifications, thus facilitating the development of more energy-efficient and environmentally friendly glass melting processes. Furthermore, studies by Yuan and Kawaji [11] have explored the integration of electric boosting with renewable energy sources, demonstrating the feasibility and environmental benefits of such hybrid systems. Additionally, research by Wang et al. [12] has examined the impact of electric boosting on the structural properties of glass, ensuring that product quality is maintained while achieving energy savings. Despite these advancements, the integration of electric boosting in industrial-scale glass furnaces faces challenges that require further investigation. The interaction between electric currents and the molten glass, the optimal placement of electrodes, and the control of thermal gradients are critical factors that need to be addressed to maximize the benefits of this technology.

Moreover, the complexity of the combustion reaction, the turbulent flow structures and the complex glass melting process require a profound comprehension of the underlying physical phenomena, demanding a gradual sophistication in model development. McConnels and Goodson [13] introduced a simplified furnace model, addressing components such as the crown, batch, and refractory temperatures. They tackled energy equations and employed the Hottel zonal method for thermal radiation, incorporating a predetermined flow structure for the glass tank. Building on this foundation, Mase and Oda [14] utilized the combustion space method, delving into twodimensional flow and temperature structures within the glass furnace, including the batch velocity over the melt. Carvalho et al. [15-17] further advanced the field by proposing a comprehensive furnace model with submodels dedicated to the combustion space, glass tank, and batch blanket. Hoke and Marchiando [18] proposed a three-dimensional model, leveraging Fluent software to optimize burner positioning relative to the glass. More recently, three-dimensional models of glass furnaces have been implemented using commercial software. Abbassi and Khoshmanesh [19] simulated and experimentally compared a glass melting furnace divided into three components: combustion chamber, batch blanket, and glass tank, using Gambit/Fluent. Li et al. [20] employed Glass Furnace model software from Glass Service (Czech Republic) to simulate a 3D model of a glass bath combustion chamber. Additionally, Raic et al. [21] and Daurer et al. [22] enhanced a CFD model to investigate oxy-fuel glass furnaces, evaluating the impact of electric boosting and bubbling on the overall system. In the context of glass furnaces, the coupling between the combustion chamber and the glass bath emerges as a critical challenge for realistically simulating furnace operations. They use the conventional method, pioneered by Carvalho [15], that introduced an iterative procedure where the combustion chamber and glass bath are solved separately to obtain the appropriate boundary conditions at the glass free surface for the next step. However, this coupling method has inherent issues: the middle sections of the free surface simultaneously experience the maximum temperature and heat flux; in addition are required many iterations between the combustion space and the glass tank models.

The research group from the University of Genova has contributed to the development of complex fluid dynamic models for the study of components of a glass production plant, spanning from the modelling of the regenerative chamber [23], glass raw material preheating systems [24], exhaust gas recirculation systems [25,26], air staging strategies [27] to the glass movements inside the bath [28]. On the combustion front, the focus extended to the exploration of fluid dynamics associated with burners [29] and the validation of combustion models through literature test cases [30]. An innovative and robust 3D CFD model has been developed to fully coupling the combustion simulation with the glass tank, ensuring physical congruence at the free surface between heat flux and temperature [31]. This paper uses the above approach to understand the effects of increased use of electric boosting on the glass melting process.

2. Material and methods

2.1 Geometry

The study involves the simulations of a glass production plant for soda lime glass. The furnace energy consumption at 5.1 [GJ/ton], ranks on the bottom 20 to 50 % of furnaces producing flint glass. The total boosting electric input is 11 % of the total energy input. The specific pull rate of the melter is low at 2.08 [ton/m^2/day], due to the high-quality products required. The furnace is gas-fired regenerative and end-port system characterized by large dimensions (over 10 [m] of length). The combustion space exhibits an arc-shaped crown, featuring two air ports with three double impulse burners each. The inner and outer nozzle flow was defined as about 1/3 for the inner nozzle and about 2/3 for the outer nozzle. The burners are positioned parallel to the furnace axis, but inclined of a specific angle with respect to the glass free surface to better mix with the combustion air. Natural gas flows from the fuel ports at the ambient temperature, while pre-heated air from the regenerative chamber is supplied through the air port. The regenerative chambers are composed of a series of refractory bricks, located in its central part, that are responsible to store heat when hot gases from combustion flow ("hot phase") and to return it to the combustion air in the "cold phase". This process is cyclic: the exhaust gas from combustion enter from the top chamber with a still high energetic content; after several minutes the air is fed from the bottom of the chamber to reach the preheated value at the top. So, the combustion flame is generated cyclically from the left or right side, based on the side where flow the preheated air and consequently is injected the fuel. The flames are generated through a diffusive mechanism.

The glass tank, tailored for a modest molten glass production, receives raw materials through two doghouses on the right and left side, incorporating a percentage of recycled material at ambient temperature. Given the limited quantities of incoming glass, the batch blanket is confined to a small region adjacent to the doghouse. A total of twelve electrodes are installed on the bottom tank surface: six in the first melting zone and six in front of the wall the separates the refining zone (figure 1).

2.2 CFD model

The computational domain considers both the combustion chamber and the molten glass bath, each discretized using an unstructured mesh with tetrahedral elements generated in Ansys Icem CFD v17.1. Within the combustion chamber domain, which includes the air and waste gas ports and the fuel burner housings, a series of mesh densities was established. Specifically, the maximum dimension within the burner housing was set at 1 [mm], gradually expanding to 30 [mm] in the fuel mixing area with a growth rate of 1.2. To optimize accuracy, the mesh near walls was strategically clustered with prism layers to maintain a y+ value around 30, ensuring effective use of wall functions. As for the glass bath, the discretization aimed to align the mesh elements on the glass surface with those in the domain above. Starting from this surface, a prism layer consisting of 10 layers was generated to accurately capture the thermal gradient within the molten glass. The combustion chamber mesh comprises approximately 4 million elements, while the glass bath mesh consists of 1.7 million cells. These grid configurations were chosen by following a comprehensive mesh sensitivity analysis conducted in prior studies [23,31]. Figure 1 shows the mesh of the two domains.

The turbulence model employed in this study is the k-epsilon model with standard wall functions, known for delivering robust results and exhibiting high numerical stability. Combustion dynamics were addressed through a multi-species model. To capture the intricate interaction between chemistry and turbulence, the eddy-dissipation-concept model was adopted, enabling the integration of detailed chemical mechanisms. In addition to solving the energy equation, radiation effects were taken into account using the P1 model, with the gray body hypothesis. A uniform air flow was imposed from the air port at a constant preheated temperature in order to obtain the requested equivalence ratio, while the burners enforced the correct flow of fuel at ambient temperature with the given composition of natural gas. An outlet condition at atmospheric pressure was set at the exhaust gas port. The furnace walls were modeled as no-slip walls, incorporating the accurate outgoing heat flux values in various areas and the appropriate emissivity. Finally, coupled with second order resolution was used as the calculation scheme of the steady simulations.

The glass bath was characterized as a laminar fluid without radiation participation. At the inlet to the doghouse, a glass flow rate at room temperature equal to the daily production of the reference furnace was imposed. The appropriate outlet condition was applied at the throat (exit section of the tank). The lateral walls and the glass tank bottom were modelled as no-slip walls with given dispersion heat flux. To account for the thermal energy required from the chemical reactions involved in melting the glass and the accurate proportion of recycled material, a uniform negative thermal source was introduced into the domain. In addition, the electric potential model was activated to calculate the Joule heat source from the electrodes for the elecctric boosting; the appropriate electric potential difference to each electrode couple was fixed as boundary condition. Each electrodes has an exit heat flux to model their cooling system to support the material limit. The properties of the glass (density, viscosity, thermal and electric conductivity) were modelled with appropriate laws depending on temperature.

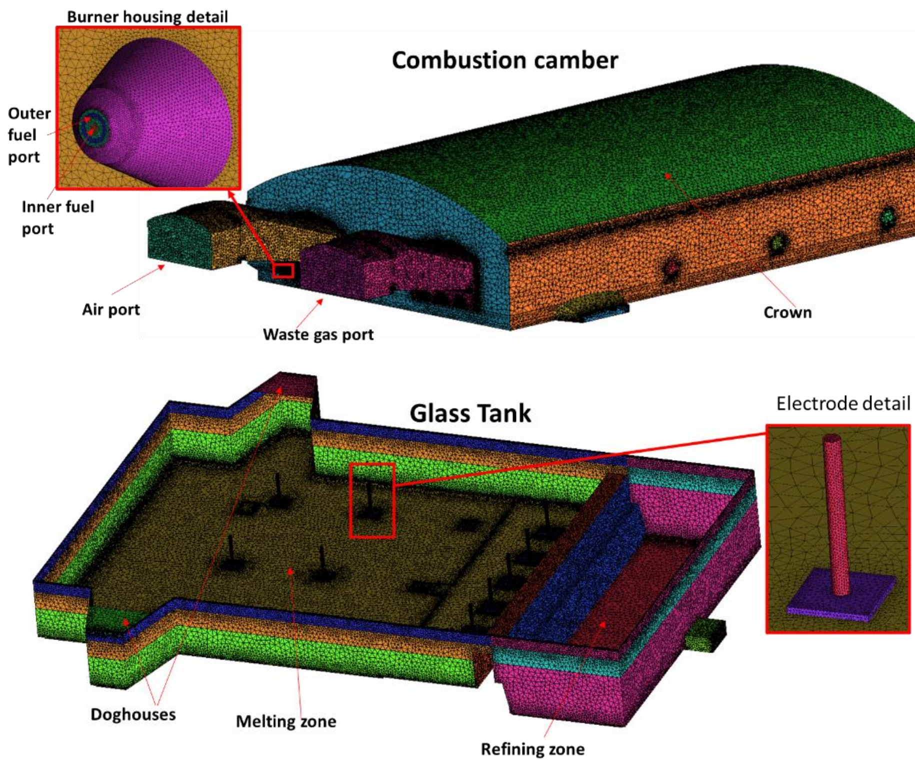

Figure 1. Mesh of the combustion chamber (upper) and glass bath (below).

The coupled simulation of combustion chamber and glass tank domains was performed. The innovative methodology, decribed in more details in an other work [31], aims to achieve a complete coupling between the two domains, by ensuring the overall thermal balance of the entire furnace and providing a correct temperature and heat flux field on the glass that depends on both combustion and convective structures.

3. Results

3.1 Validation

To show the flame structure inside the combustion chamber, in Figure 2 the volumetric rendering of OH in the combustion chamber is depicted as the primary indicator of the flame (on the left), in addition to the streamline originated from the air port and burners, color-coded to represent temperature (on the right).

In this visualization, the development of the flame through diffusion, resulting from the complex mixing of pre-heated combustion air from the regenerative chamber and fuel jets emanating from the burners can be observed. The presence of the flame is detected in regions with the highest concentration of OH radicals. This is evident in the area immediately downstream of the burners, after the mixing process and it extend up to approximately the wall into the glass tank that split the melting and the refining zone. It is a good practice to design a furnace where the maximum flame falls in this region i.e. two thirds of the glass bath length. From the streamline view it is evident that the flame interacts with the exhaust gases path giving a flow recirculation towards the back wall and the crown, with the typical U-structure of the end-port regenerative glass furnace. The flow recirculation towards the crown is typical from the burner type used and it is necessary to reduce the pollutant emission by allowing the best mixing to complete the formation reaction of CO_2 rather than CO and decreasing the local maximum temperature for the NOx reduction.

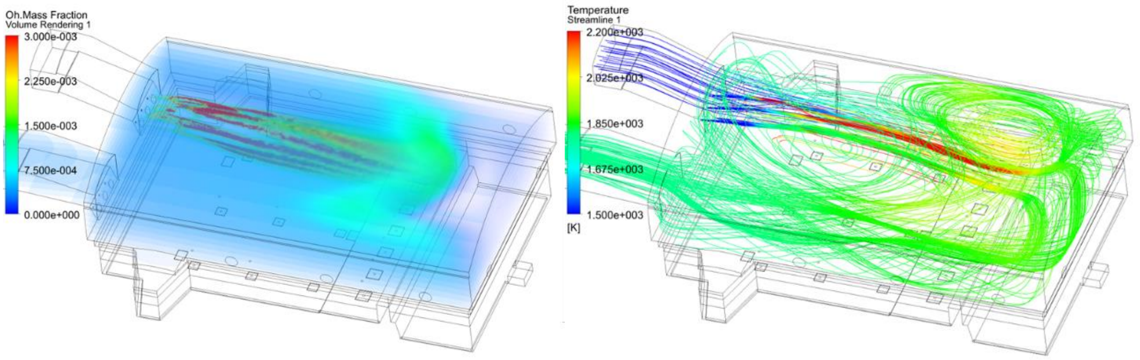

Figure 2. Volume rendering of OH in the combustion chamber (left) and streamline in the combution chamber from the air port and burners color-coded with the temperature (right) – baseline C1.

In order to validate the model, the measured temperatures with appropriate thermocouples on the combustion chamber crown and on the glass tank bottom were compared with those obtained from CFD simulations, as shown in Figure 3.

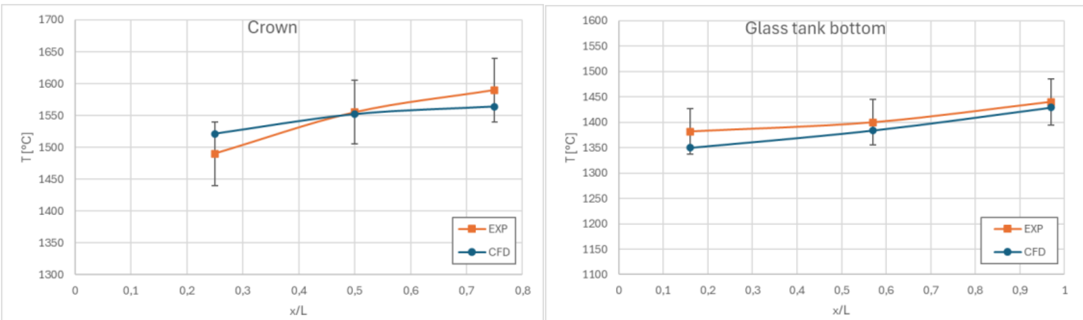

Figure 3. Comparison between CFD and experiment of the temperature measured in the crown and glass tank bottom for the baseline C1.

By comparing the temperature values, it was possible to verify the accuracy of the CFD model; the temperature trends on both the crown and the glass tank bottom are in good match, with maximum errors always below 2.5%. Additionally, the obtained values are inside the measure uncertainty, represented by error bars in the graphs. The numerical values always fall within the confidence interval of the measurements.

3.2 Analysis with different electric boosting

To evaluate the effects of increased electric boost on the glass melting process, a case was simulated with a doubled percentage of power supplied through the electrodes and compared to the baseline case, by keeping the total input energy (combustion + electricity) constant. Table 1 shows the distribution of energy supplied through combustion and electrodes for the two cases.

Figure 4 shows the streamlines originating from the air port and burners, color-coded with the temperature, for the case C2. Compared to the baseline case (shown in Figure 1), it is evident that the maximum flame extension has decreased and tends to recirculate towards the crown well before reaching the splitting wall into the glass tank. In fact, with a lower fuel massflow rate and the unchanged burner geometry, the fuel jet enters at a lower velocity and it spreads less.

Table 1. Dataset of the simulated cases.

Case	Combustion power	Electric power
C1 (Baseline)	87.5%	12.5%
C2	75%	25%

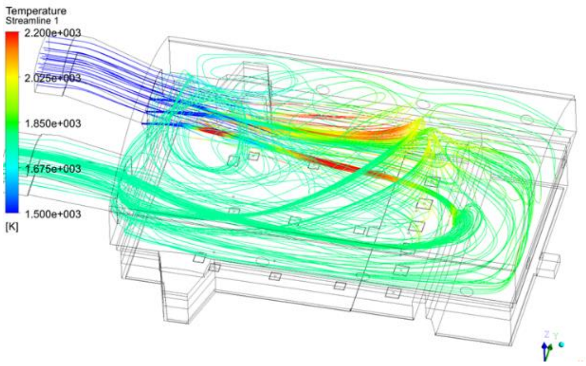

Figure 4. Streamline in the combustion chamber from the air port and burners color-coded with the temperature – Case C2.

In Table 2, the different pollutant emissions at the waste gas port are reported. Despite the furnace operates with the same equivalence ratio, a higher amount of oxygen was observed in the exhaust gases of case C2, indicating slightly more incomplete combustion. This results in a shift of the smoke point (the point in the O2-CO diagram where at low O2 the CO increases exponentially), leading to a reduction in CO emissions. Moreover, in case C2, the CO_2 emitted into the atmosphere was reduced by over 22%, mainly due to the lower amount of fuel used, thanks to the greater integration of energy supplied by the electrodes. In case this electrical energy is obtained from renewable sources, the overall environmental impact of the system is strongly reduced.

Table 2. Pollutant emissions of the exhaust gases for the two cases.

Pollutant	C1	C2
O_2 [%]	2.4	2.8
CO [ppm]	100	64
CO_2 [ton/day]	44.71	34.67

In Figure 5, the free glass surface heat flux and temperature distributions for the two cases are compared. The fully coupled approach offers the main advantage over conventional methods of being able to simultaneously and accurately calculate both quantities. From the comparison, it is clearly evident that in case C2, less heat flux is passed from the combustion chamber to the glass melt; consequently, the temperatures on the free surface are approximately 20 [°C] lower. However, in both cases, the hot spots are located in the final refining section, while the maximum heat flux (situated at about two-thirds of the melt) occurs slightly earlier in case C2.

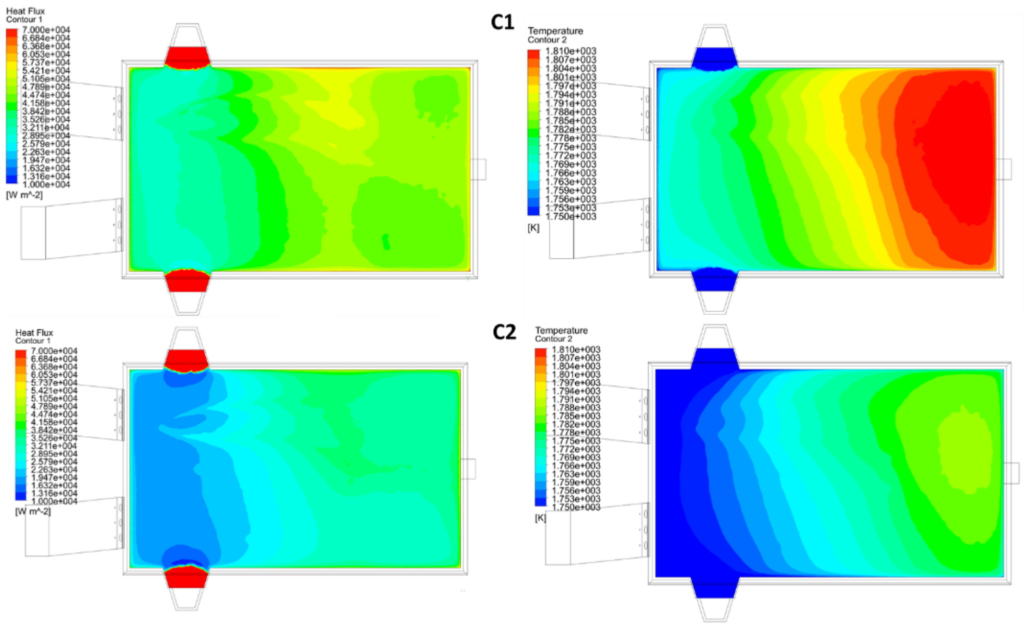

Figure 5. Contour of the thermal flux (left) and temperature (right) on the free glass surface - comparison between C1 (upper) and C2 (below)

Table 3 shows the percentage contribution of the thermal flux relative to the total thermal input flux (both combustion and electric).

Table 3. Main contribution of the thermal flux percentage in the glass furnace with respect to the total thermal inlet flux for the two cases.

Thermal contribution	C1	C2
Q_{fumes} [%]	-73.6	-60.4
$Q_{to\text{-}glass}$ [%]	42.7	30.5
$Q_{glass,out}$ [%]	34.6	34.2

It can be observed that less thermal power reaches the glass melt from the combustion chamber in case C2, because the portion of energy provided by combustion is reduced; consequently, the exhaust gases also leave the furnace with a lower residual thermal power. Despite these differences, the thermal power of the molten glass exiting the throat remains almost unchanged due to the increased use of electrodes.

To analyze the effects on the glass melt in more detail, Figure 6 shows a comparison of the mid-plane glass temperatures for the two cases, with the addition of the surface velocity streamlines. In case C2, the temperature near the surface is lower than in the base case, while at the bottom a higher temperature is observed. In case C2 a higher temperature homogeneity in the melt is found. This is due to better mixing induced by the electrodes, which create a more pronounced and beneficial flow recirculation in the melting zone upstream and downstream of the electrode rows.

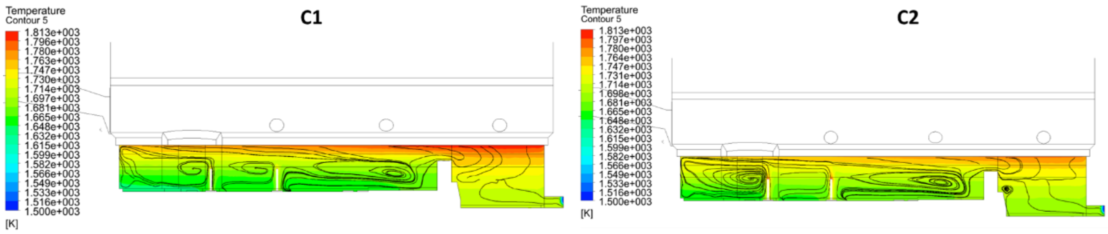

Figure 6. Contour of temperature and velocity surface streamline in the middle plane of the glass tank.

Finally, to understand the quality of the molten glass the residence time of the glass into the tank is a reference indicator; the highest the better. Figure 7 shows the Gaussian distribution of the residence times of the glass particles in the melt before exiting through the throat and be delivered to the glass channels.

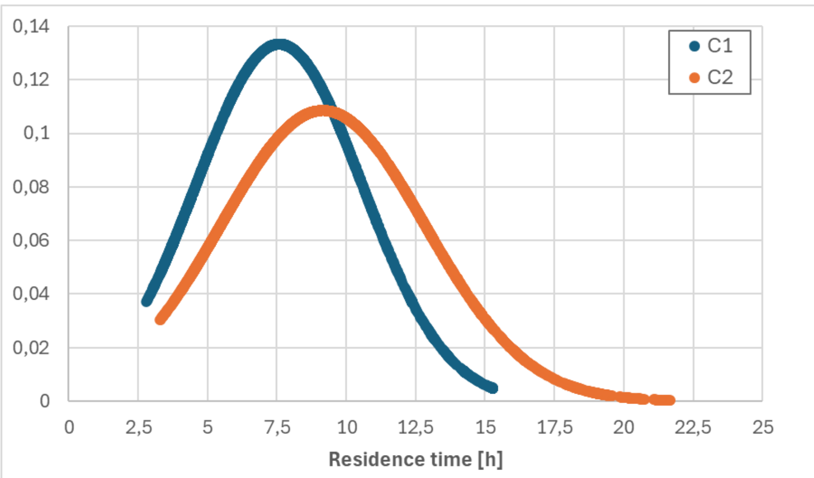

Figure 7. Gaussian distribution of the residence time in the molten glass of the fluid particles.

This graph shows that the residence time in case C2 is increased by approximately 25%. This improvement is primarily due to the stronger recirculation observed previously, due to the greater energy provided by the electrodes. A longer residence time ensures a higher quality final product by increasing the time available for the melting and homogenization of solid glass particles from the doghouses.

4. Conclusions

The developed CFD model allows to simulate a real glass furnace for combustion, thermal, and fluid dynamic with very detailed analysis. The fully coupled approach between the combustion chamber and the glass tank developed by the authors enables precise calculation of the furnace heat fluxes and the glass melt temperature. This model has been validated by comparing experimentally measured temperature values with those obtained from the CFD model.

Detailed analyses were conducted on the main differences in the flame generated and the related pollutant emissions in the base case compared to the more electrified case. Specifically, compared to the base case, it was possible to reduce greenhouse gas emissions by over 22%, leading to a consequent improvement in environmental impact. Additionally, the enhanced electrical boosting improved the glass melting process by increasing convective movements, residence time and consequently, the quality of the glass as a final product. The results obtained confirm that an increased support of electrical boosting to the melting process can be beneficial from both energetical and environmental issues and it can also support a better glass quality. The optimisation of both furnace design and operation requires the systematic use of the simulation approaches like the one developed by the authors.

Acknowledgment

This research was developed within the project “Network 4 Energy Sustainable Transition – NEST” funded under the National Recovery and Resilience Plan (NRRP), Mission 4 Component 2 Investment 1.3 - Call for tender No. 1561 of 11.10.2022 of Ministero dell’Università e della Ricerca (MUR); funded by the European Union – NextGenerationEU.

References

[1] Schmitz, A.; Kaminski, J.; Scalet, B.M.; Soria, A. “Energy consumption and CO2 emissions of the European glass industry”. Energy Policy 2011, 39, 142–155
[2] Koshelnik, A.V. “Modelling operation of system of recuperative heat exchangers for aero engine with combined use of porosity model and thermos-mechanical model”. Glass Ceram. 2008, 65, 9–10, 301–304.
[3] Selvaray, J.; Varun, V.S.; Vishwam, V. “Waste heat recovery from metal casting and scrap preheating using recovered heat”. Procedia Eng. 2014, 97, 267–276.
[4] Fathi, M.; Saray, R.K.; Checkel, M.D. “The influence of Exhaust Gas Recirculation (EGR) on combustion and emissions of n-heptane/natural gas fueled Homogeneous Charge Compression Ignition (HCCI) engines”. Appl. Energy 2011, 88, 4719–4724.
[5] Spliethoff, H.; Greul, U.; Rüdiger, H.; Hein, K.R. “Basic effects on NOx emissions in air staging and reburning at a bench-scale test facility”. Fuel 1996, 75, 560–564.
[6] Staiger, B.; Unterberger, S.; Berger, R.; Hein, K.R. “Development of an air staging technology to reduce NOx emissions in grate fired boilers”. Energy 2005, 30, 1429–1438.
[7] Kuzyak VA. “Electric boosting of glass heating in flame tank furnaces. Glass Ceram”. 1958; 15(11): 586–91.
[8] Verheijen, R.; Giezen, C.; Teunissen, A. “Reduction of CO2 Emissions in Glass Furnaces through Electric Boosting”. Journal of Cleaner Production 2018, 172, 1422-1431.
[9] Abenojar, J.; Martínez, M.A.; Velasco, F. “Advances in Electrode Materials for Electric Boosting in Glass Furnaces”. Materials Science and Engineering: B 2020, 255, 114567.
[10] Müller, S.; Hoffmann, G.; Behrens, M. “CFD Modeling of Electric Boosting in Glass Melting Furnaces: Impact on Melt Homogeneity and Energy Efficiency”. Computational Thermal Sciences 2017, 9(2), 101-112.
[11] Yuan, C.; Kawaji, M. “Integration of Electric Boosting with Renewable Energy in Glass Melting Processes”. Renewable Energy 2019, 138, 712-722.
[12] Wang, J.; Zhang, Y.; Li, H. “Impact of Electric Boosting on the Structural Properties of Glass”. Journal of Materials Processing Technology 2016, 229, 1-10.
[13] McConnell, R.R.; Goodson, R.E. “Modeling of glass furnace design for improved energy efficiency”. Glass Technology 1979, 20 (3), 100– 106.
[14] Mase, H.; Oda, K. “Mathematical model of glass tank furnace with batch melting process”. Journal of Non-Crystalline Solids 1980, 38–39, 807–812.
[15] Carvalho, M.G. “Computer simulation of a glass furnace”. PhD Thesis, London University, 1983.
[16] Carvalho, M.G.; Nogueira, M. “Modelling fluid flow and heat transfer in an industrial glass furnace”. Annual ESPRIT Conference, Kluwer, Dordrecht, Netherlands, 1990, 530–543.
[17] Carvalho, M.G.; Nogueira, M.; Wang, J. “Mathematical modeling of glass melting industrial process”. 17th International Congress on Glass 1995, 6, 69–74, Beijing, China.

[18] Hoke, B.C.; Marchiando, R.D. "Using combustion modeling to improve glass melt model results". 4th International seminar on mathematical simulation in the glass melting, Horni Becva, Czech Republic, 1997, 87–95.
[19] Abbassi, A.; Khoshmanesh, K. "Numerical simulation and experimental analysis of an industrial glass melting furnace". Applied Thermal Engineering 2008, 28(5-6), 450-459.
[20] Li, L.; Lin, H.J.; Han, J.; Ruan, J.; Xie, J.; Zhao, X. "Three-dimensional glass furnace model of combustion space and glass tank with electric boosting". Materials Transactions 2019, 60(6), 1034-1043.
[21] Raič, J.; Gaber, C.; Wachter, P.; Demuth, M.; Gerhardter, H.; Knoll, M.; Hochenauer, C. "Validation of a coupled 3D CFD simulation model for an oxy-fuel cross-fired glass melting furnace with electric boosting". Applied Thermal Engineering 2021, 195, 117166.
[22] Daurer, G.; Raič, J.; Demuth, M.; Gaber, C.; Hochenauer, C. "Detailed comparison of physical fining methods in an industrial glass melting furnace using coupled CFD simulations". Applied Thermal Engineering 2023, 232, 121022.
[23] Cravero, C.; Marsano, D. "Numerical simulation of regenerative chambers for glass production plants with a non-equilibrium heat transfer model". WSEAS Trans. Heat Mass Transf. 2017, 12, 21–29.
[24] Cravero, C.; De Domenico, D.; Leutcha, P.J.; Marsano, D. "Strategies for the numerical modelling of regenerative pre-heating systems for recycled glass raw material". Math. Model. Eng. Probl. 2019, 6, 324–332.
[25] Cogliandro, S.; Cravero, C.; Marini, M.; Spoladore, A. "Simulation strategies for regenerative chambers in glass production plants with strategic exhaust gas recirculation system". IJHT Int. J. Heat Technol. 2017, 35, S449–S455.
[26] Cravero, C.; De Domenico, D. "The Use of CFD for the Design and Development of Innovative Configurations in Regenerative Glass Production Furnaces". Energies 2019, 12, 2455.
[27] Cravero, C.; De Domenico, D.; Marsano, D. The Use of Uncertainty Quantification and Numerical Optimization to Support the Design and Operation Management of Air-Staging Gas Recirculation Strategies in Glass Furnaces. Fluids 2023, 8, 76.
[28] Cravero, C.; Marsano, D. "Numerical Simulation of Melted Glass Flow Structures inside a Glass Furnace with Different Heat Release Profiles from Combustion". Energies 2023, 16(10), 4187.
[29] Cravero, C.; Lamberti, A.; Poggio, L. "CFD Prediction of a Double Impulse Burner for Glass Furnaces". Energies 2023, 16, 4275.
[30] Cravero, C. Lamberti A.; Marsano, D.; Milanese, G. "Numerical investigation of turbulent fuel jet diffusion and its influence on the auto-igniting diffusive flame development". J. Phys.: Conf. Ser 2024.
[31] Cravero, C. Marsano, D.; Milanese, G. "A CFD model for the direct coupling of combustion process and glass melting flow simulation in glass furnaces". In preparation.